CHAPTER IV
RESULTS AND DISCUSSION

In this chapter, details will be separated into two parts. The first part was the results and discussion from using boron-doped diamond thin film electrode (As-deposited BDD) for the determination of thiol-containing drugs. The results obtained from batch system and flow injection analysis will be presented respectively. For the second part, the working electrode was changed from As-deposited BDD electrode to anodized boron-doped diamond thin film (Anodized BDD) electrode for the analysis of homocysteine. The results obtained were categorized in the same steps as shown in the first part. Additionally, HPLC results will be discussed as well at the end of this part.

4.1 Boron-Doped Diamond Thin Film Electrodes for Thiol-Containing Drugs Analysis Coupled with Flow Injection Analysis System

4.1.1 Cyclic Voltammetry

Cyclic voltammetry was initially used as means of examining and comparing the electrochemical signal of two electrodes (BDD electrode and GC electrode) for the analysis of captopril and tiopronin. Figure 4.1a details the voltammetric response obtained at BDD electrode when it was placed in a 0.1 M phosphate buffer (pH 9) solution, containing 1 mM captopril whilst Figure 4.1b details the response of the GC electrode under analogous conditions. Analysis of the cyclic voltammograms recorded prior to the addition of captopril reveals that the response at each electrode produced no appreciable oxidative signals over the potential range studied (0.0 to +1.4 V). Furthermore, a comparison of the background currents observed at each electrode reveals that the BDD electrode exhibited a lower capacitance consistent (~ 10 times) than GC electrodes. Upon the introduction of captopril to the solution the response at the BDD electrode showed a new well defined electrochemical signal emerging at +0.5 V which obtained a current plateau at +0.8 V. In contrast, the captopril response obtained at the GC electrode showed only increase in the oxidation current at +0.7 V. This current continued to rise

with increasing potential but unlike the BDD electrode no defined oxidation wave was observed. Upon reversal of the scan direction no new reductive processes were observed in the potential range studied at each electrode. This was consistent with the electrochemically oxidized species of captopril undergoing a chemically irreversible reaction.

For tiopronin, the similar results were obtained when using 2 mM tiopronin in a 0.1 M phosphate buffer (pH 8) solution. The data was shown in Figure 4.2a and 4.2b, respectively.

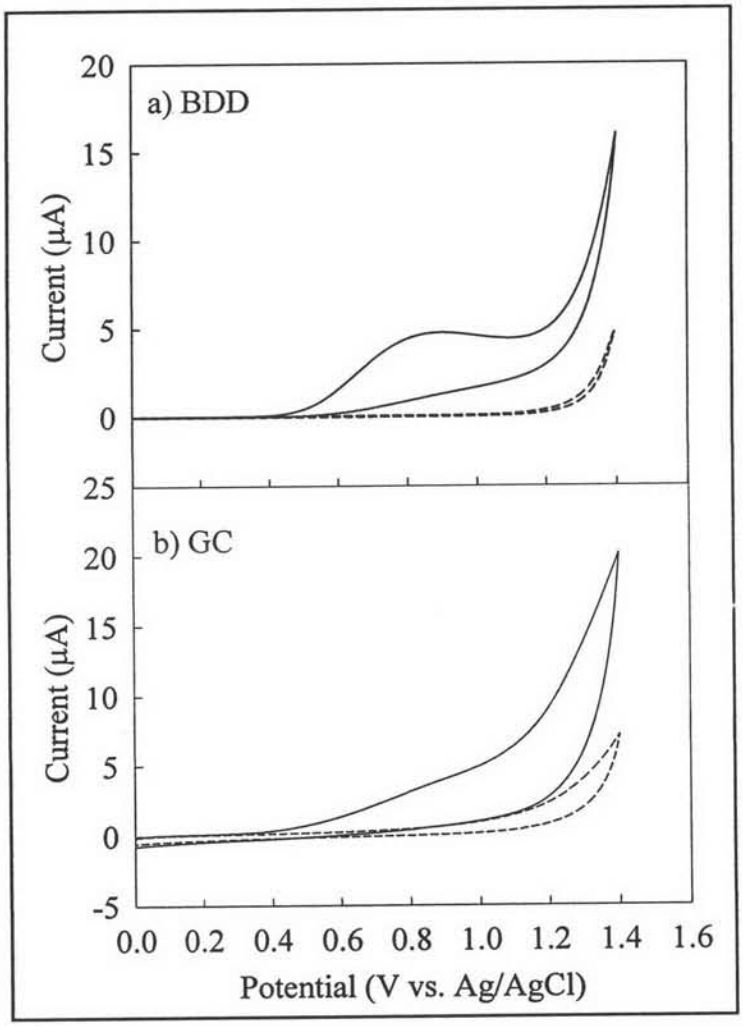

Figure 4.1 Cyclic voltammograms for a) BDD and b) GC versus Ag/AgCl in 1.0 mM captopril in 0.1 M phosphate buffer pH 9 (solid lines) and 0.1 M phosphate buffer pH 9 (dashed lines) Sweep rate, 50 mV/s; area of electrode, 0.07cm^2.

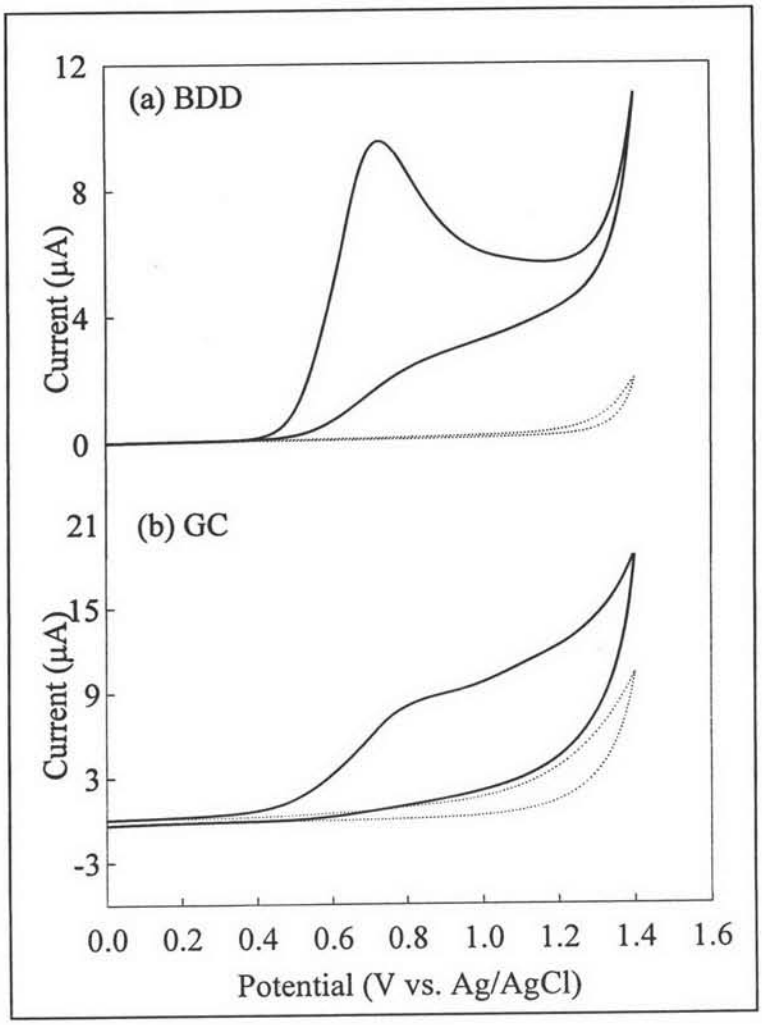

Figure 4.2 Cyclic voltammograms for a) BDD and b) GC versus Ag/AgCl in 2.0 mM tiopronin in 0.1 M phosphate buffer pH 8 (solid lines) and 0.1 M phosphate buffer pH 8 (dashed lines) Sweep rate, 50 mV/s; area of electrode, 0.07cm^2.

4.1.2 Effect of pH on the Electrochemical Behavior of Thiol-Containing drugs

In order to obtain the optimum electrochemical responses of thiol-containing drugs, it was important to examine the effect of buffer pH. Phosphate buffer, 0.1 M, was used as the supporting electrolyte for investigating the electrochemical property of thiol-containing drugs. The experiments were performed

at pH 2.5, 5.0, 6.0, 7.0, 8.0, and 9.0. The results obtained showed that thiol-containing drugs can be oxidized in neutral and alkali media. In the case of acidic buffer, the BDD electrode provided an ill-defined cyclic voltammograms while the GC electrode provided a featureless cyclic voltammograms. For captopril and tiopronin, the peak potential was shifted towards to more negative when the pH value increased as shown in Table 4.1 and 4.2, respectively. This remark can be explained using the electrooxidation of sulfur-containing compounds at BDD electrode [138]. It involved the dissociation of the proton from the thiol group, followed by the electrochemical oxidation of captorpil (or tiopronin) anion. So at higher pH value, captopril and tiopronin was easy to loose the proton and to produce more stable reduced form. The highest oxidation current peak with the maximum S/B ratios was obtained from using phosphate buffer pH 9 for captopril and buffer pH 8 for tiopronin, respectively. Thus, these pHs were selected for all subsequent experiments.

Table 4.1 Comparison of electrochemical data obtained from the cyclic voltammograms of 1 mM captopril for the diamond electrode at various pH values.

pH	E_p^{ox} (vs. Ag/AgCl)	I_p^{ox} (μA)
2.5	-	-
5.0	-	-
6.0	0.96	2.78
7.0	0.95	3.26
8.0	0.90	3.89
9.0	0.87	5.12

Table 4.2 Comparison of electrochemical data obtained from the cyclic voltammograms of 2 mM tiopronin for the diamond electrode at various pH values.

pH	E_p^{ox} (vs. Ag/AgCl)	I_p^{ox} (μA)
2.5	-	-
5.0	-	-
6.0	0.94	4.63
7.0	0.857	4.98
8.0	0.812	5.69
9.0	0.79	5.02

- no peak

4.1.3 Scan Rate and Concentration Dependence

In order to verify that these oxidative reactions were diffusion controlled, a study into the effects of scan rate on the electrochemical signal was undertaken. The equation used for describing the relationship between the current signal and scan rate for totally irreversible reaction was shown below [6]:

$$i_p \text{ (diffusion)} = (2.99 \times 10^5) n(\alpha n_a)^{1/2} A C_0^* D_0^{1/2} \upsilon^{1/2}$$

The corresponding voltammetric responses varied with scan rate with the current plateau increasing linearly with the square root of the scan rate. Such dependence indicated that the oxidation of captopril (or tiopronin) was indeed diffusion controlled. Figure 4.3 and 4.4 showed the cyclic voltammograms recorded

during variation of the scan rate for the BDD electrode. It can be seen that peak current (μA) was linearly proportional to the square root of the scan rate (V/ s) within the range 0.01 to 0.3 V/ s. The linear regression analysis yields $R^2 > 0.9990$. From the voltammogram, it was found that the peak potential shifted positively with increasing sweep rate, as expected for an irreversible process, and the linearity suggest that the reaction involves a diffusing species.

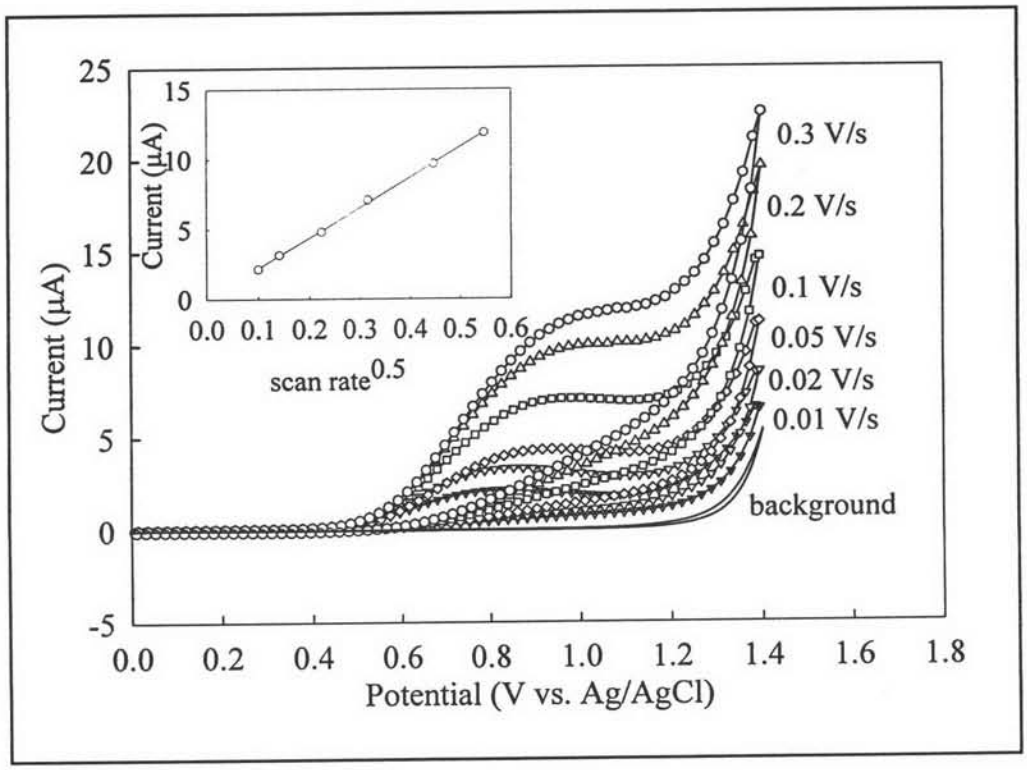

Figure 4.3 Cyclic voltammogram for 1 mM captopril in 0.1 M phosphate buffer (pH 9) at boron-doped diamond electrode for a series of potential sweep rates; area of electrode, 0.07 cm^2. The calibration curve of relationship between current (μA) and $(\text{sweep rate})^{0.5}$ was also in the inset of this figure.

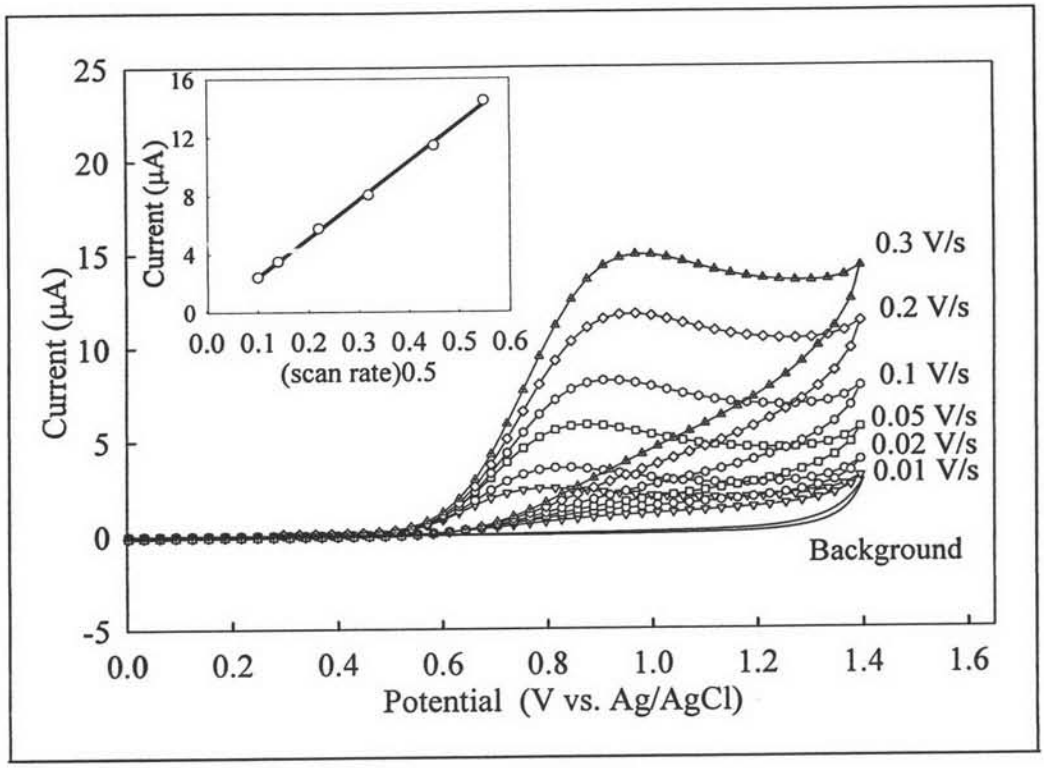

Figure 4.4 Cyclic voltammogram for 1 mM tiopronin in 0.1 M phosphate buffer (pH 8) at boron-doped diamond electrode for a series of potential sweep rates; area of electrode, 0.07 cm^2. The calibration curve of relationship between current (μA) and $(\text{sweep rate})^{0.5}$ was also in the inset of this figure.

Next, the analytical utility of using the BDD electrode was examined. The variation in the voltammetric currents was analyzed as a function of the captopril (or tiopronin) concentrations from 0.025 - 20 mM. The response of the BDD electrode was found to be linear over the concentration range 0.05 - 3 mM for captopril and from 0.05 – 10 mM for tiopronin and produced a limit of detection at S/B ≥3 of 50 μM for both drugs. The data was shown in Figures 4.5 and 4.6.

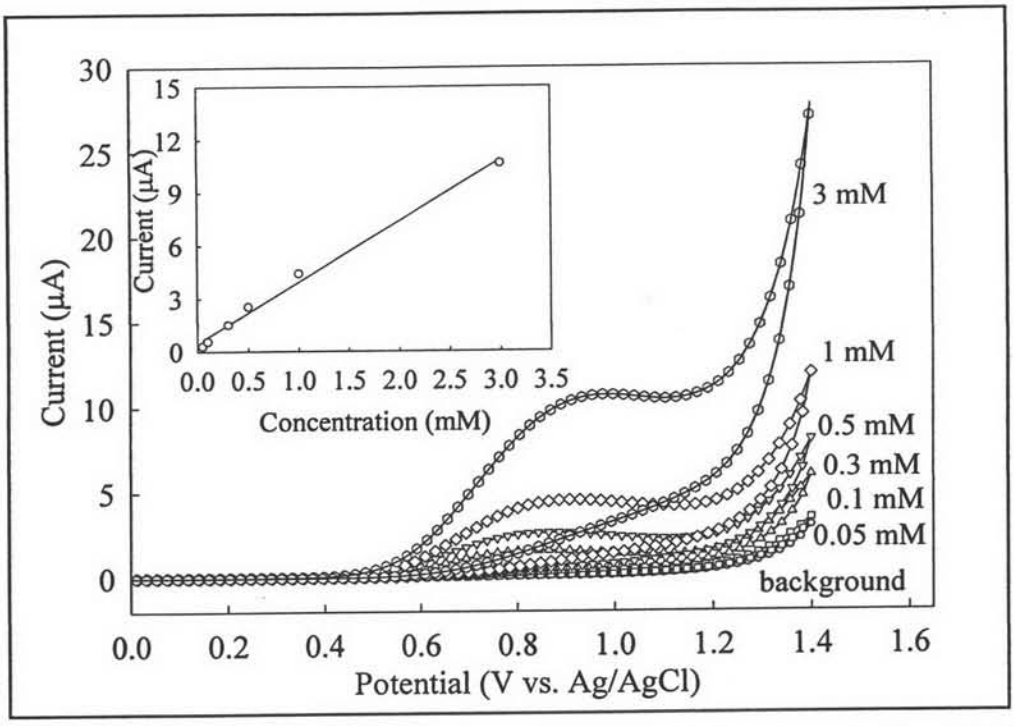

Figure 4.5 Cyclic voltammogram for captopril in 0.1 M phosphate buffer (pH 9) at boron-doped diamond electrode for a series of captopril concentrations. The potential sweep rate was 50mV/ s; area of electrode, 0.07cm^2. The calibration curve was shown in the inset.

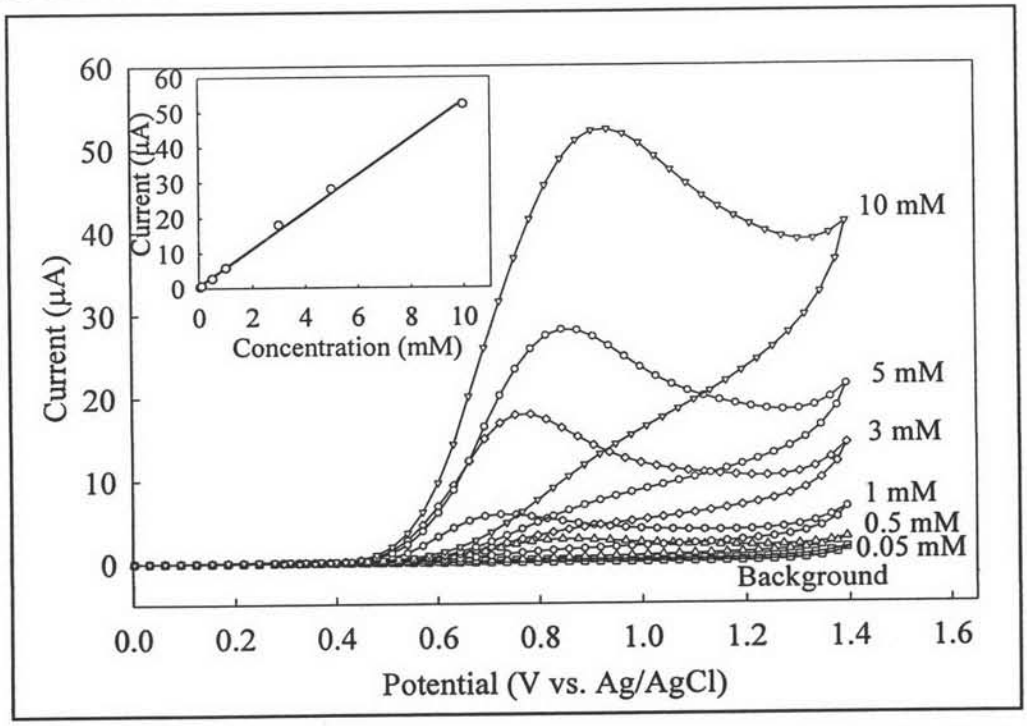

Figure 4.6 Cyclic voltammogram for tiopronin in 0.1 M phosphate buffer (pH 8) at boron-doped diamond electrode for a series of captopril concentrations. The potential sweep rate was 50mV/ s; area of electrode, 0.07cm^2. The calibration curve was shown in the inset.

4.1.4 Flow Injection with Amperometric Detection

4.1.4.1 Hydrodynamic Voltammetry

Hydrodynamic voltammetry was a suitable method to determine the appropriate potential applied to the FIA/amperometic detection. In this study, standard solution of thiol-containing drugs was repetitively injected while the FIA/amperometry operating potential was increased from 0.5 V to 1.0 V in 0.1 V increments. Figure 4.7a displayed the hydrodynamic voltammogram of 20 μL injections standard solution containing 100 μM captopril in 0.1 M phosphate buffer (pH 9), using 0.1 M phosphate buffer (pH 9) as the carrier solution. Each datum represents the average of four injections. The absolute magnitude of the background current at each potential was also shown for comparison. When the applied potential increased the current response of captopril also increased, and none reached the maximum value. Hence, the S/B ratio was calculated from the Figure 4.7a at each point to create a graph as a function of S/B ratios and applied potential (Figure 4.7b) to obtain the maxima potential point. To get the best sensitivity and signal to noise ratio, +0.9 V was chosen as an optimal detection potential for captopril.

Using the same procedure, the maximum S/B ratio at 0.8 V was achieved for tiopronin. Hence, this potential was selected for quantitative amperometric detection in FIA experiments for tiopronin. The data was illustrated in Figure 4.8.

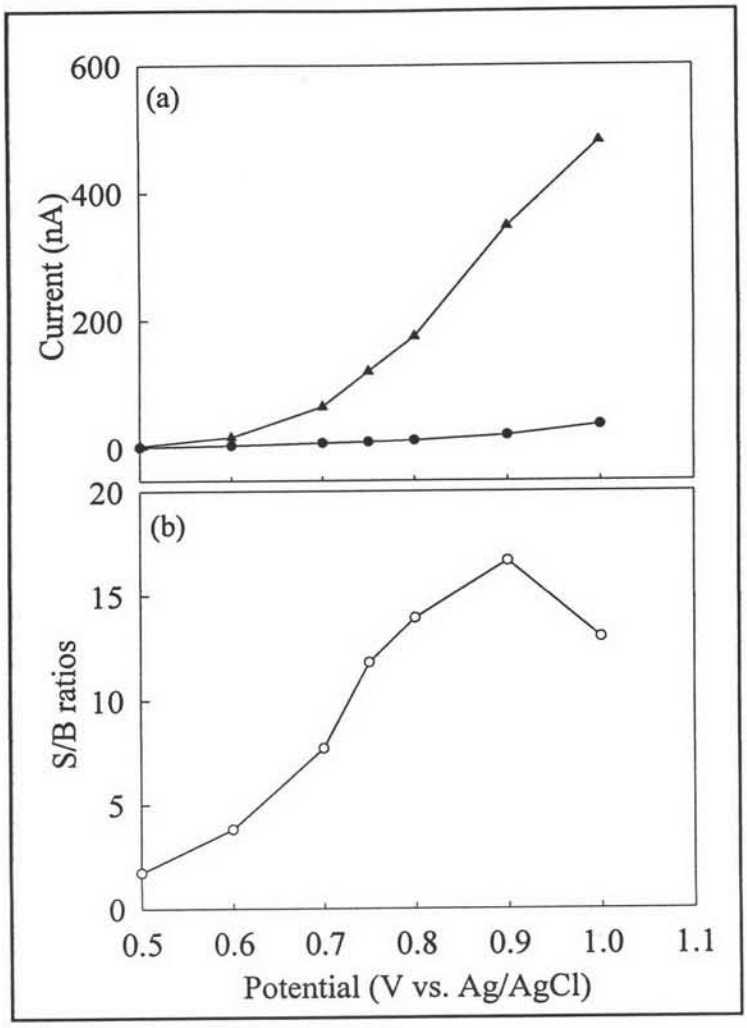

Figure 4.7 (a) Hydrodynamic voltammogram of (-•-) 0.1 M phosphate buffer (pH 9, background current) and (-▼-) 100 μM of captopril in 0.1 M phosphate buffer (pH 9) with four injections of analysis, using 0.1 M phosphate buffer (pH 9) as a carrier solution. (b) Hydrodynamic of signal- to- background ratio. The flow rate was 1 mL/ min.

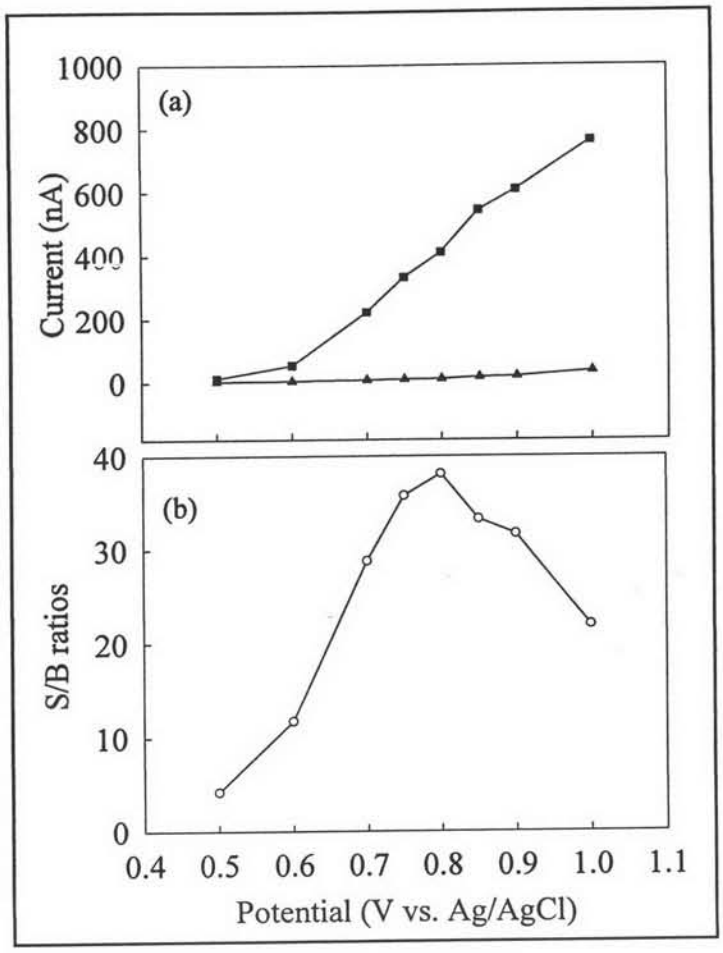

Figure 4.8 (a) Hydrodynamic voltammogram of (-▲-) 0.1 M phosphate buffer (pH 8, background current) and (-■-) 100 μM of tiopronin in 0.1 M phosphate buffer (pH 8) with four injections of analysis, using 0.1 M phosphate buffer (pH 8) as a carrier solution. (b) Hydrodynamic of signal- to- background ratio. The flow rate was 1 mL/ min.

4.1.4.2 Flow Injection Analysis

After optimizing the suitable detection potential for the FIA procedure, amperometric measurements were carried out in phosphate buffer containing different thiol-containing drugs concentration in order to obtain the analytical curve. Figure 4.9 and Figure 4.10 illustrated the FI current-time response for different captopril concentrations and tiopronin concentration, respectively. A

linear relationship between the current values (at +0.9 V) obtained and the captopril concentrations exhibited from 100 to 0.5 μM (see inside Figure 4.9). This plot could be represented by the equation (I_{anodic}/nA) = x[captropril]) with a correlation coefficient of 0.999. To higher concentrations than 100 μM occurred the deviation of linearity. The detection limit was 10 nM (S/N = 3, Figure 4.11). For tiopronin, an excellent FIA results were also obtained using BDD electrode at the detection potential of +0.8 V. Well-defined signals were obtained at all concentration from 5 nM to 500 μM. The linear dynamic range increased with increasing the concentration from 50 to 0.5 μM, R^2= 0.9992, as shown in the inset of Figure 4.10. In addition, a detection limit for S/N = 3 was determined. It can be seen that at optimal detection potential, the BDD electrode could detect a tiopronin concentration as low as 10 nM as displayed in Figure 4.12.

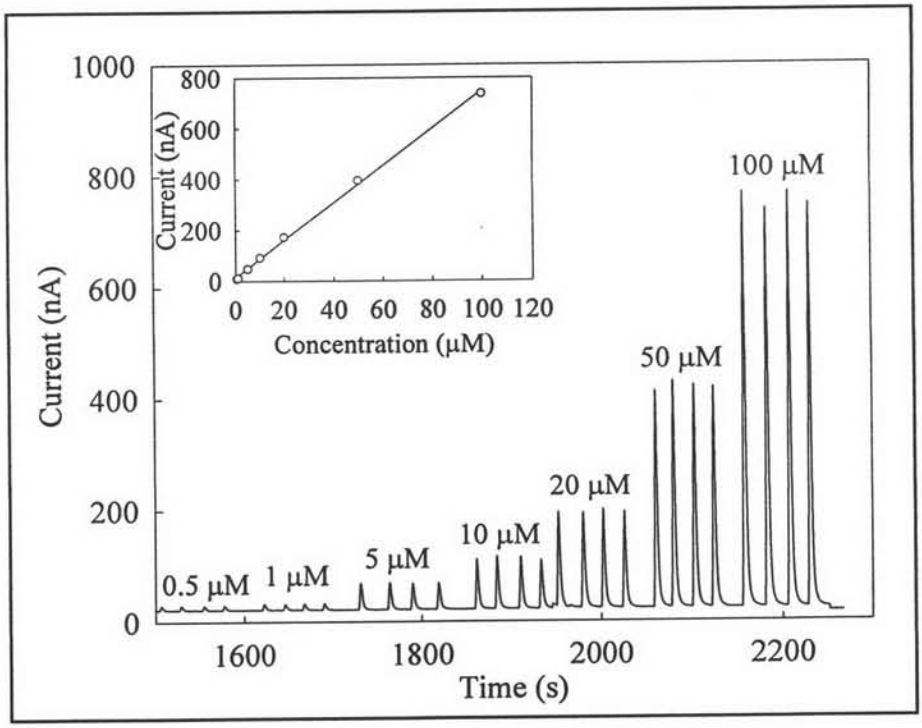

Figure 4.9 Flow injection analysis with amperometric detection results for a diamond electrode using 20-μL of captopril at various concentrations. The mobile phase was 0.1 M phosphate buffer (pH 9) at a flow rate of 1 mL/min. The calibration curve was shown in the inset.

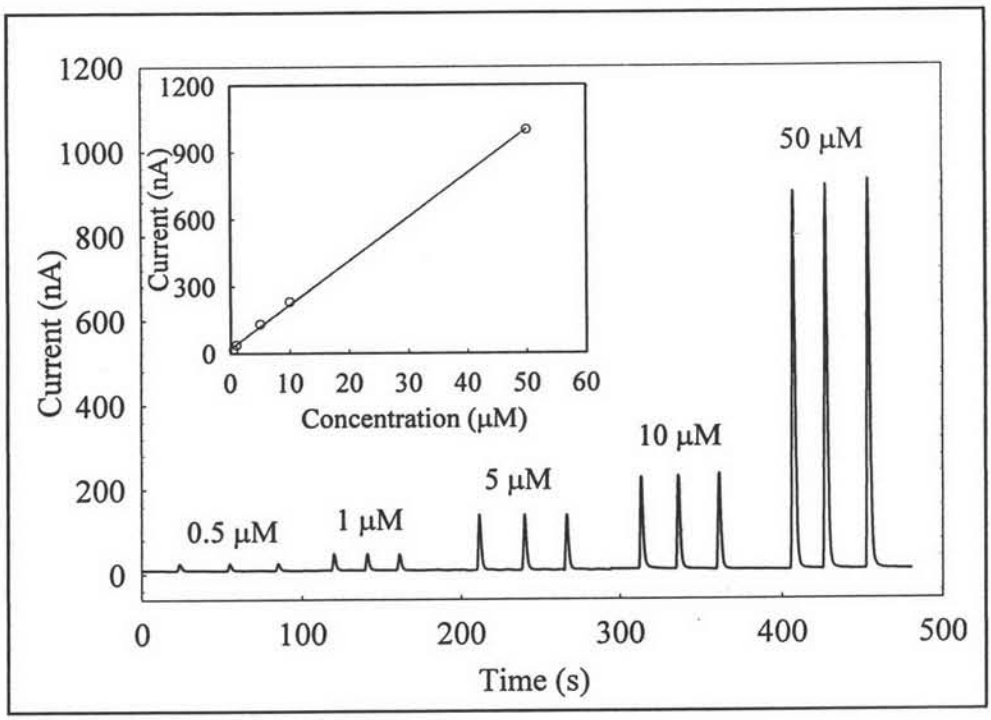

Figure 4.10 Flow injection analysis with amperometric detection results for a diamond electrode using 20-μL of tiopronin at various concentrations. The mobile phase was 0.1 M phosphate buffer (pH 8) at a flow rate of 1 mL/min. The calibration curve was shown in the inset.

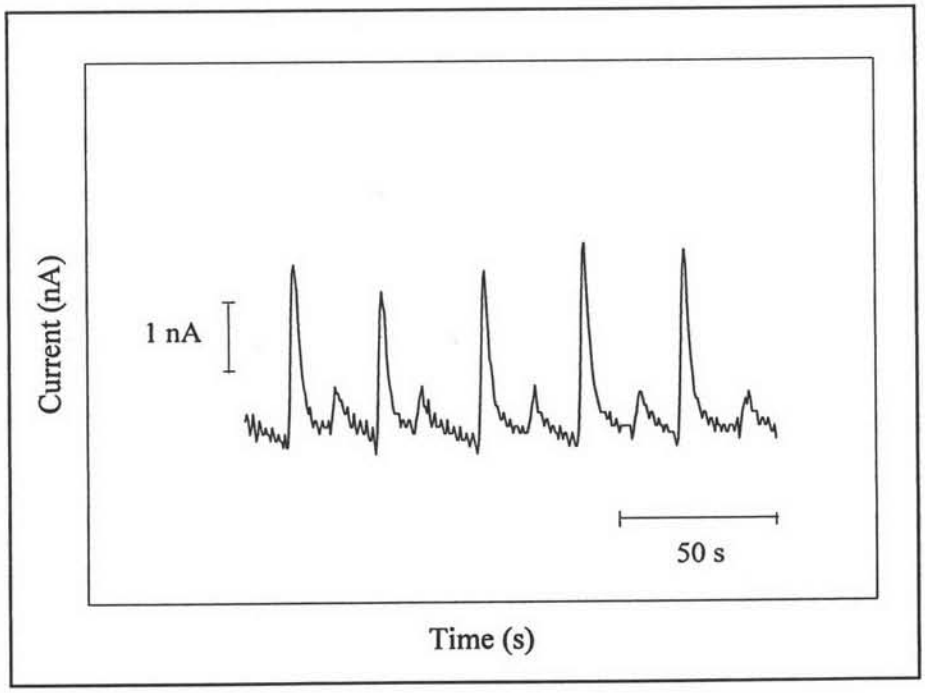

Figure 4.11 Flow injection with amperometric detection results for 10 nM captopril in 0.1 M phosphate buffer (pH 9). The flow rate was 1 mL/min.

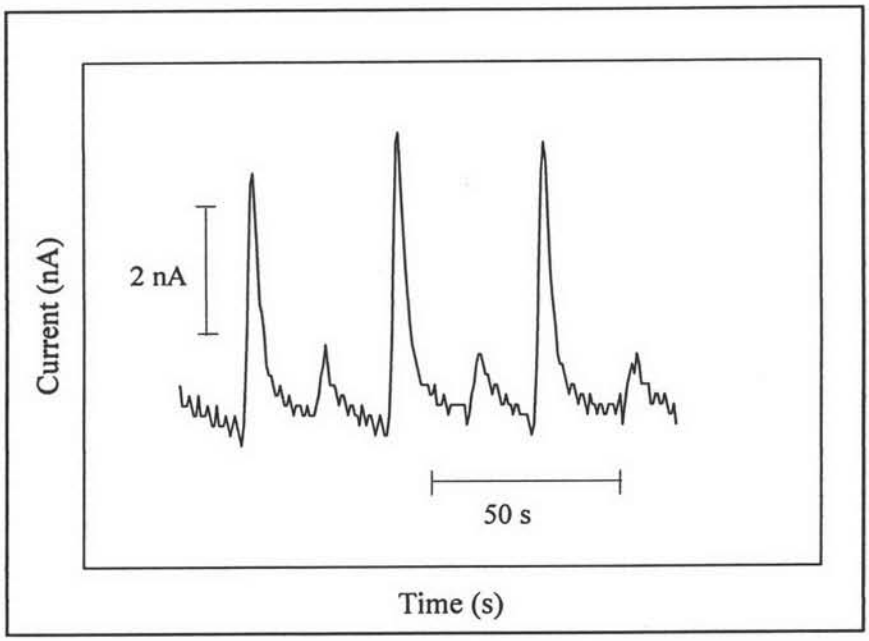

Figure 4.12 Flow injection with amperometric detection results for 10 nM tioproninin 0.1 M phosphate buffer (pH 8). The flow rate was 1 mL/min.

4.1.5 Applications: Quantitative Determination of Thiol-Containing Drugs in Pharmaceutical Preparations.

In order to investigate the analytical capability of proposed method, the BDD electrode was applied to the analysis of captopril in the formulation. In this work, we examined the accuracy of the proposed method for determination of captopril in pharmaceuticals by the method of the standard addition (Figure 4.13). The results were summarized in Table 4.3, including the repeatability data (n = 2). The recoveries of the added captopril, ranging from 95.85 to 109.29 % were also shown in Table 4.4.

The precision of the method was obtained on the basis of intra-assay. Three concentrations of added solution (0.00, 0.43, 1.74 μg / mL) were chosen. Results obtained from ten injections were within 1.21-2.15 % of the relative standard deviation (RSD). The RSD values for day-to-day assays of captopril were also investigated. It has been found in the same laboratory within one week that the RSD values did not exceed 2 %.

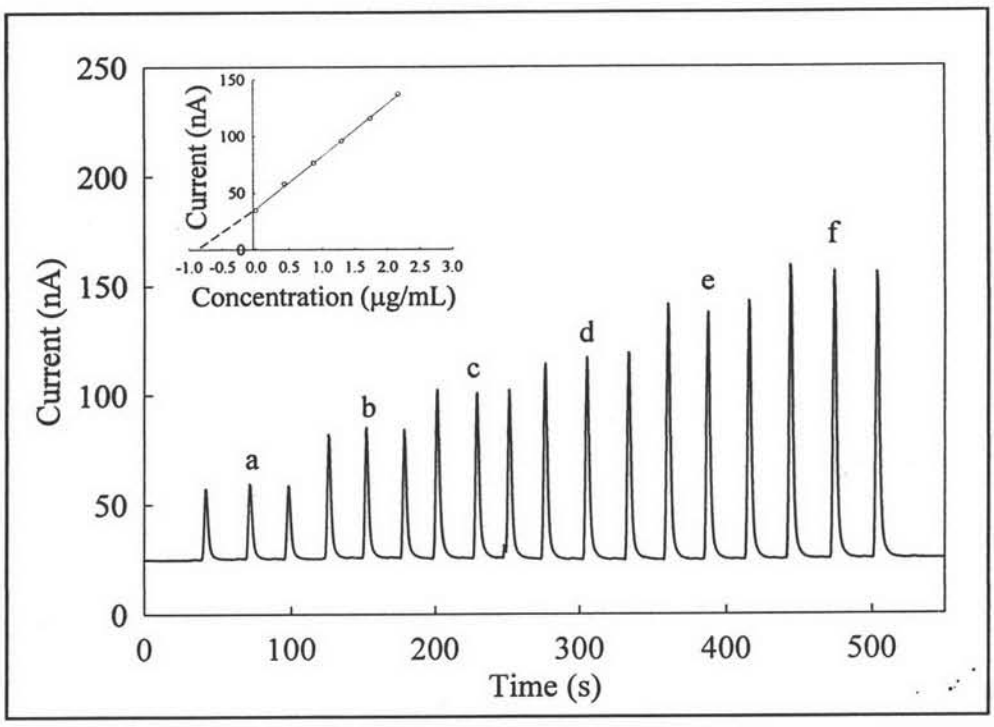

Figure 4.13 Flow injection analysis results for determination of captopril in commercially available tablets. Using the standard addition for the added captopril: (a) 0.00 mg/mL, (b) 0.43 mg/mL, (c) 0.87 mg/mL, (d) 1.30 mg/mL, (e) 1.74 mg/mL, (f) 2.17 mg/mL.

Table 4.3 Precision and accuracy in the determination of commercially available tablet dosage form.

Drug	Sample Number	Found
Captopril (12.5 mg/tablet)	1	12.89
	2	12.90

Table 4.4 Recovery of captopril tablet sample with amperometric detection using diamond electrode applied to flow injection system (n=2)

Amount added (μg/mL)	Amount found (μg/mL)	Percent of recovery (%)
0.43	0.47±0.00	109.29±0.02
0.87	0.91±0.14	105.62±3.41
1.30	1.25±0.01	95.85±0.24
1.74	1.77±0.06	101.93±0.72
2.17	2.15±0.02	98.99±0.17

Moreover, this proposed electrode was also applied to the analysis of tiopronin in formulation. We examined the accuracy of the method for determination of tiopronin in pharmaceuticals by the method of the standard addition as shown in Figure 4.14. Linear least square calibration curve provided a slope of 21.07 nA /μM (sensitivity) and correlation coefficient of 0.996. Relative error compared with the claimed amount was lower than 4%. The recoveries of the added tiopronin ranged between 96.5 and 108.3%, were obtained as shown in Table 4.5. At lower concentration, it was non-linear, with the slope gradually decreasing when the concentration grows. We expected that it was due to the inexistence of a plateau, result from hydrodynamic voltammogram, the current became quite potential-dependent and any uncompensated IR drop in the cell can contribute to the blending.

Another possible cause can be found in Figure 4.4: the anodic wave suffered displacement to more positive potential with increasing concentration. This non-linearity can be caused overestimation at low concentrations to expected values, followed by underestimation at the upper end. The tiopronin content of the drug calculated from this calibration plot (102.8 ± 0.03 mg per tablet, $n = 2$) was found to be in satisfactory agreement with the labelled amount of 100 mg per tablet. The precision of the method was obtained on the basis of intra-assay. Three concentrations of added solution (0.00, 0.98, 1.63 μg/mL) were chosen. Results obtained from 10 injections were within 1.10–1.62% of the relative standard deviation (RSD) as illustrated in Figure 4.15. Moreover, the RSD values between two analyses were also investigated. It was found that the RSD did not differ more than 1.5%.

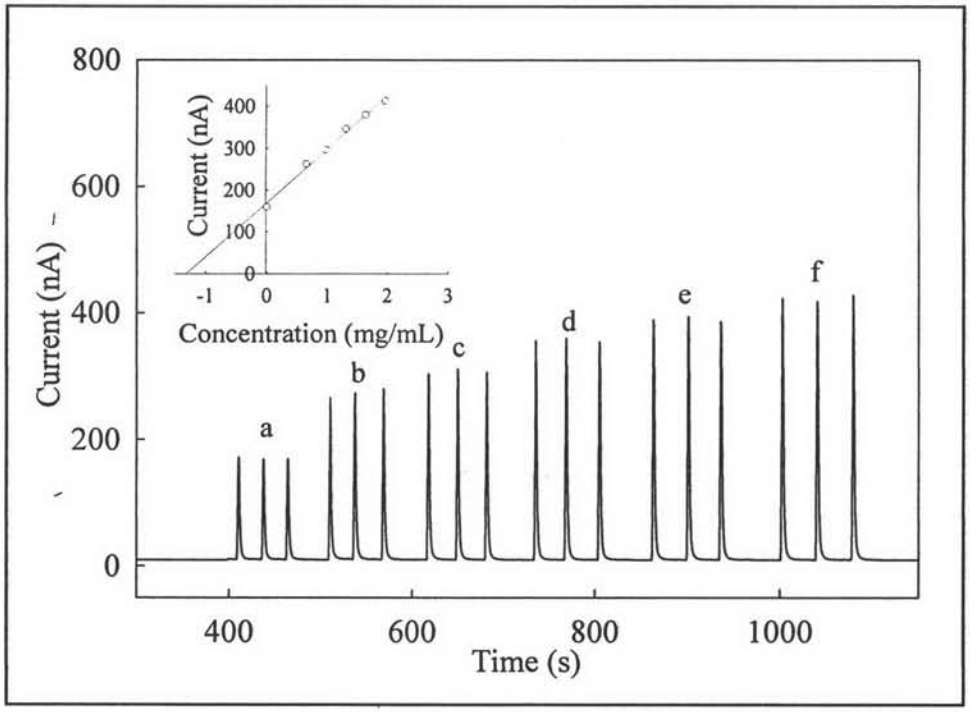

Figure 4.14 Flow injection analysis results for determination of tiopronin in commercially available tablets. Using the standard addition for the added captopril: (a) 0.00 mg/mL, (b) 0.65 mg/mL, (c) 0.98 mg/mL, (d) 1.31 mg/mL, (e) 1.63 mg/mL, (f) 1.96 mg/mL.

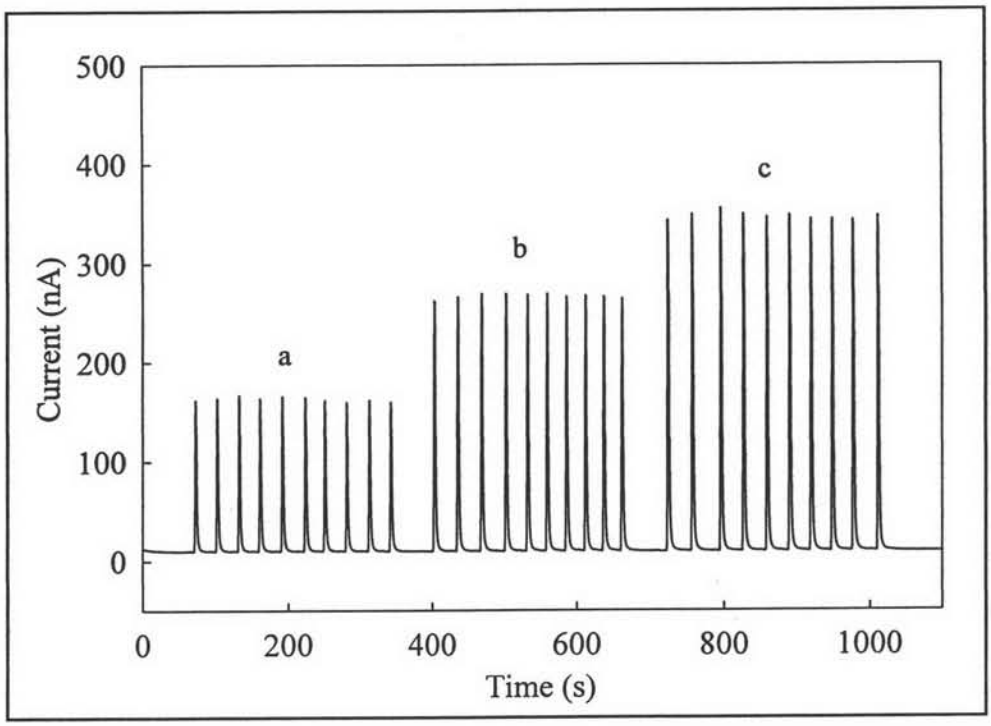

Figure 4.15 Precision results from flow injection - amperometric detection of tiopronin at concentrations of : a, 0 μg/mL; b, 0.98 μg/mL; and c, 1.63 μg/mL (n = 10).

Table 4.5 Recovery of tiopronin tablet samples with amperometric detection using boron-doped diamond thin film electrode applied to flow injection system (n=3)

Amount of tiopronin tablet sample added (μg/mL)	Amount of tiopronin tablet sample found (μg/mL)	Percent of Recovery
0.65	0.7 ± 0.02	108.3 ± 3.6
0.98	1.04 ± 0.07	105.2 ± 6.7
1.31	1.35 ± 0.04	103.2 ± 2.8
1.63	1.62 ± 0.01	99.6 ± 0.4
1.96	1.89 ± 0.002	96.5 ± 0.1

4.16 Comparison to the Other Methods

Table 4.6 summarized data from the other methods for determination of tiopronin compared with the proposed method. It was found that using the BDD electrodes with amperometric FIA gave the similar wide linear dynamic range to other methods (two orders of magnitudes). Interestingly, the proposed method provided a very low detection limit of 10 nM, because the BDD electrode exhibited very low background current and noise signals. It also resulted in very high sensitivity. This outstanding performance of the BDD electrode made it attractive for using as working electrode in FIA system for analysis of tiopronin.

Table 4.6 Comparison of data for tiopronin determination

Method	Linear dynamic range (μM)	Detection limit (μM)	Precision (percent RSD)	Reference
Flow injection fluorometric	0.8-20	0.098	1.0 (at 1 μM)	121
Flow injection chemiluminescent	0.1-70	0.036	2.6 (at 1 μM)	122
Liquid chromatography with electrochemical detection	5-20	0.710	-	127
Chemiluminescent HPLC coupled with flow injection	1-100	0.80	4.8 (at 1 μM)	128
Diamond thin film electrode applied to flow injection analysis	0.5-50	0.010	1.1 (at 1 μM)	a

(-) No report

a This proposed method.

4.17 Summary

This is the first use of BDD thin film electrodes for the electroanalysis of thiol-containing drugs (captopril and tiopronin). It was found that BDD electrodes exhibited excellent performance for the oxidative detection of thiol-containing drugs. Well-defined voltammograms were obtained at the BDD electrode, which exhibited high sensitivity, and demonstrated significant advantages over the GC electrode, because of its superior electrochemical properties. Moreover, well-defined sweep rate dependent cyclic voltammograms were also obtained. It indicatedthat the electrochemical process of thiol-containing drugs on BDD electrode was controlled by the diffusion of the species. The pH dependence of thiol-containing drugs oxidation showed that, at the diamond electrode, a well-defined response can be obtained in an alkaline media, while a response can not be obtained at a GC electrode in either acidic or basic media. In addition, the use of the BDD electrode was a simple analytical procedure, because no chemical modification was required. Cleaning of the electrode with time was not necessary due to the long-term stability of the BDD electrode response. The outstanding capabilities of the BDD electrode were demonstrated by coupling with FIA. The results indicated that captopril and tiopronin can be detected amperometrically without derivatization or the use of a pulse waveform. The advantage of the BDD electrode was that it was able to achieve a highly stable and sensitive response with simple amperometric detection. Application of the proposed method for determination of thiol-containing drugs in commercially available tablet forms showed that this method was precise, accurate, and very sensitive.

4.2 The Electrochemical Oxidation of Homocysteine at Anodized Boron-Doped Diamond Thin Film Electrodes with Amperometric HPLC

4.2.1 Cyclic Voltammetry

The oxidation of homocysteine in alkaline solution at an as-deposited BDD electrode was previously investigated [138]. In the present work, we have compared the oxidative responses obtained for as-deposited BDD and anodized BDD electrodes, both in acidic and alkaline media as shown in Figure 4.16. The confirmation was performed that in alkaline media, as-deposited boron-doped diamond electrodes yielded an anodic wave corresponding to thiol oxidation at 0.6 V. Interestingly, at the anodized diamond electrode, an additional wave was found at 1.4 V. It should be noted here that the potential sweep for the as-deposited BDD surface was reversed at +1.2 V, because higher potentials oxidize the surface irreversibly. The first oxidation wave can be explained on the basis that, in alkaline media, the deprotonation of homocysteine occurred. In the acidic solution, at an anodized electrode (Figure 4.16B), only one voltammetric oxidation peak was obtained, at a potential of 1.4 V. No response was observed at the as-deposited BDD electrode in acidic media.

Similar results have been explained recently in work carried out with glutathione on the basis of attractive electrostatic interactions between the negatively charged anodized surface and the positively charged substrate, since the solution pH was below the isoelectric point [163]. In contrast, with as-deposited diamond, the surface was positively charged, and the electrostatic interaction would be repulsive. It has been conclusively shown that the oxidation mechanism at anodically treated diamond electrodes in acidic solution involved oxygen atom transfer [163]. This type of mechanism was originally proposed by Johnson *et al.*, who studied the oxidation of sulfur-containing amino acids and peptides at Bi (V)-doped PbO_2 film electrodes in acidic media [164]. A similar mechanism was also proposed for the $Bi_3Ru_3O_{11}$ electrode [165]. These findings have been explained with a mechanism in which a prerequisite was the anodic discharge of H_2O to produce adsorbed OH radicals, which were the immediate source of O-atoms transferred to the oxidation products [164]. This

oxidation reaction proceeded through an initial one-electron step to form radicals (•SR), which subsequently undergo further oxidation, with transfer of oxygen from hydroxyl radicals at the electrode surface to produce RSO_3H [163].

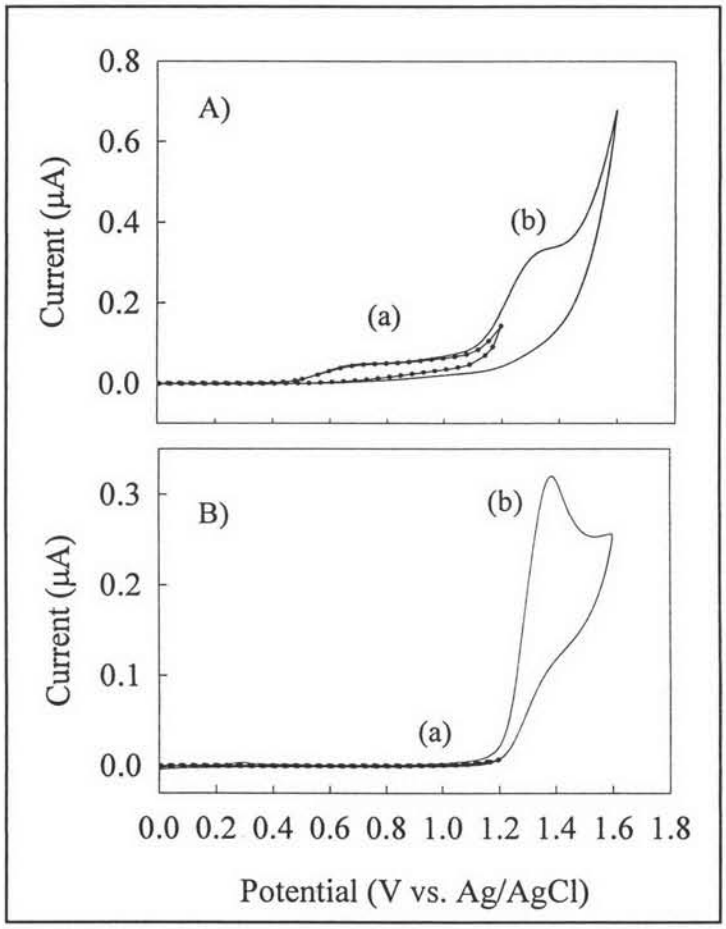

Figure 4.16 (A) Cyclic voltamograms for 1 mM homocysteine in 0.1 M phosphate buffer (pH 9) at (a) an as-deposited boron-doped thin film electrode (dotted line) and (b) an oxidized (anodized) boron-doped thin film electrode (solid line). (B) Cyclic voltamograms for 1 mM homocysteine in 0.05 M phosphate buffer (pH 2.7) at (a) an as-deposited boron-doped thin film electrode (dotted line) and (b) an oxidized boron-doped thin film electrode (solid line).

4.2.2 Concentration and Scan Rate Dependence

The oxidation peak current was measured at the anodized BDD electrode for the concentration range of 0.2 to 2 mM homocysteine in 0.05 M phosphate solution (pH 2.7) at the BDD. Based on a series of cyclic voltammograms in which the concentration of homocysteine was varied from 0.2 mM to 2 mM (Figure 4.17), a linear regression analysis of peak current versus concentration was obtained, with excellent linearity from 0.2 to 2 mM ($R^2 > 0.999$). At concentrations greater than 2 mM, passivation-type behavior was obtained, probably due to electrode fouling. The potential scan rate dependence was also investigated in this experiment (Figure 4.18). From the voltammograms, it was found that the peak potential shifted positively with increasing sweep rate, as expected for an irreversible process, and the current response was linear with the square root of the sweep rate, indicating that the reaction involved a diffusing species.

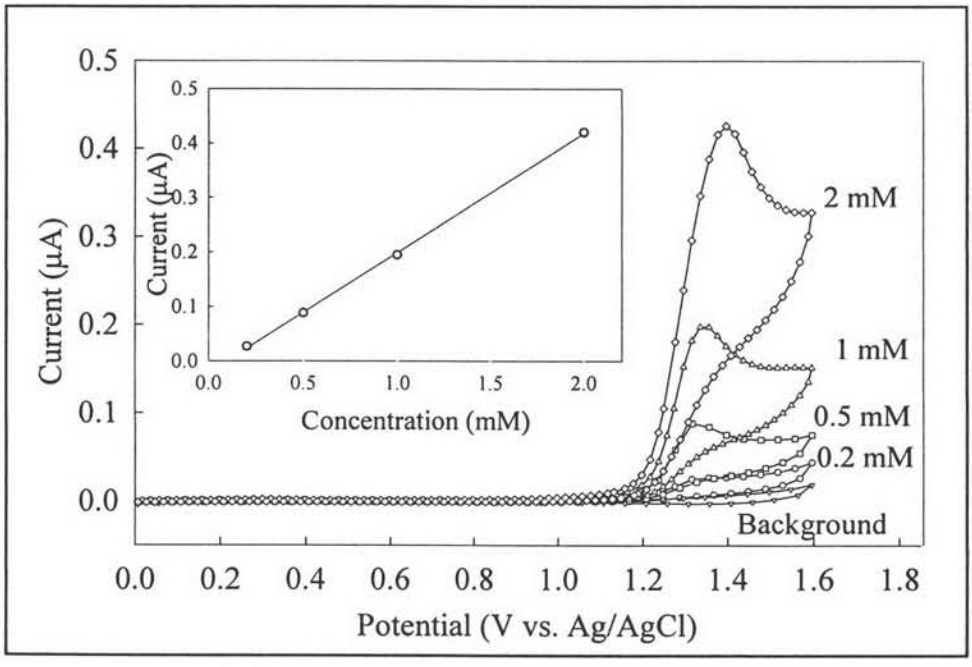

Figure 4.17 Cyclic voltammogram for homocysteine in 0.1 M phosphate buffer (pH 2.7) at anodized boron-doped diamond electrode for a series of homocysteine concentrations. The potential sweep rate was 50mV/ s; area of electrode, 0.07cm^2. The calibration curve was shown in the inset.

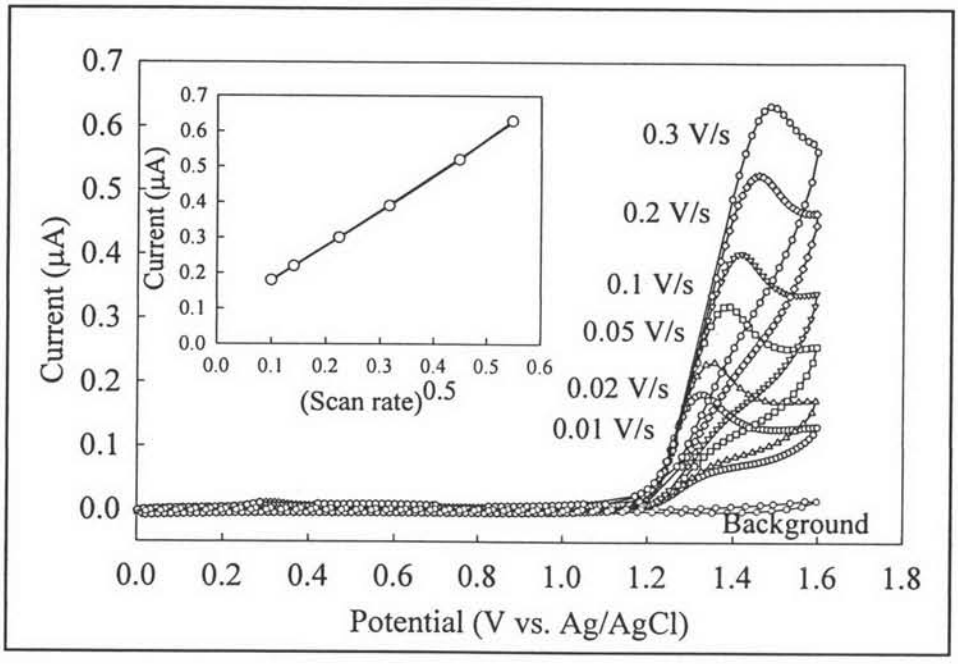

Figure 4.18 Cyclic voltammogram for 1 mM homocysteine in 0.1 M phosphate buffer (pH 2.7) at anodized boron-doped diamond electrode for a series of potential sweep rates; area of electrode, 0.07 cm^2. The calibration curve of relationship between current (μA) and $(\text{sweep rate})^{0.5}$ was also in the inset of this figure.

4.2.3 Hydrodynamic Voltammetry

To obtain an optimal potential for the amperometric detection, both in FIA and HPLC measurements, the hydrodynamic voltammetric behavior of both reduced and oxidized aminothiols were studied. Figure 4.19 showed the hydrodynamic voltammetric *i–E* curves obtained at the anodized BDD electrode for 20 μL injections of homocysteine, homocystine, cysteine, cystine, methionine, reduced glutathione and oxidized glutathione (each 20 μM) in 50 mM phosphate solution (pH 2.7). A solution of 3% acetonitrile in 50 mM aqueous phosphate solution (pH 2.7) was used as the carrier. The maximal potential was about 1.9 V for all compounds. It was observed that, at lower potentials (1.1–1.4 V), –S–S– compounds (cystine, homocystine and oxidized glutathione) produced a very high oxidative response, whereas –SH compounds (cysteine, homocysteine and reduced

glutathione) produced less current. When the potential was higher (1.5–1.8 V), the –SH compounds began to produce a comparable oxidative current, and the oxidative response for the –S–S– compounds increased more slowly. At a potential of 2 V, both –SH compounds and –S–S– compounds produced a similar response. From these results, it can be concluded that the selected detection potential was very critical in determining the sensitivity. As already mentioned, anodized boron-doped diamond can be operated at very high potentials, because it exhibited strong resistance to oxidative attack. Hence, to obtain very high sensitivity results, an amperometric detection potential of 1.9 V could be chosen. However, we found that this potential produced very high background currents, and a stable background current was reached only slowly. Therefore, it was necessary to make a trade-off between time-consuming background current stabilization and increased sensitivity. Thus, in practice, we selected a potential of 1.6 V for the FIA and HPLC amperometric detection.

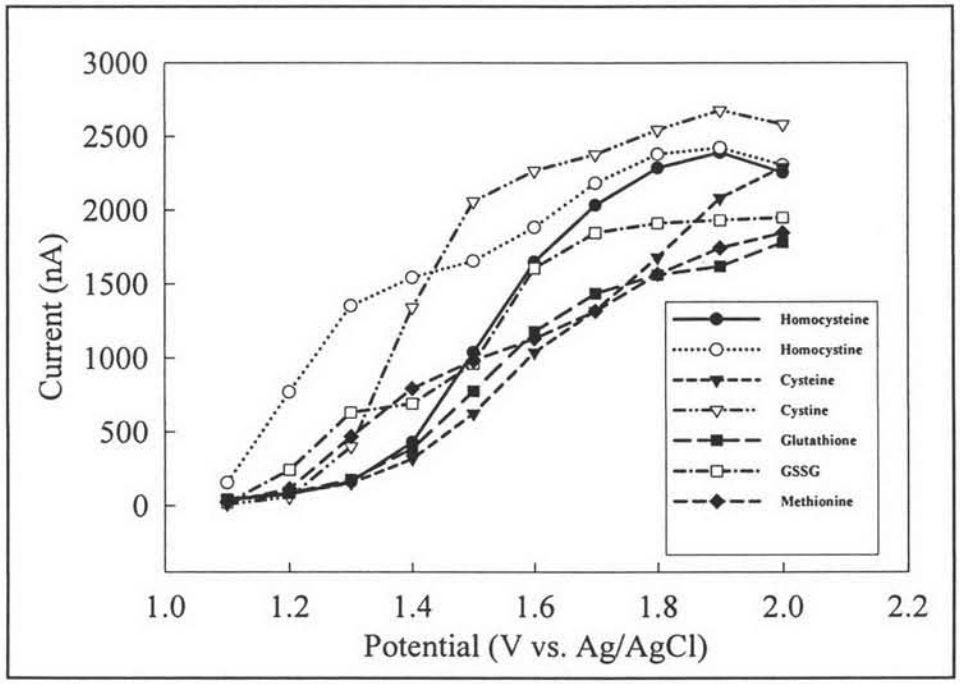

Figure 4.19 Hydrodynamic voltammograms at the anodized BDD electrode for 20 μL injections of homocysteine, homocystine, cysteine, cystine, methionine, reduced glutathione and oxidized glutathione (each 20 μM) in 3% acetonitrile–0.05 M phosphate buffer (pH 2.7). The flow rate was 1 mL/ min.

4.2.4 Flow Injection Analysis

Recently, a number of papers have appeared concerning the use of boron-doped diamond electrodes in FIA for the determination of organic compounds. In the present work, we also obtained excellent FIA results using anodized boron-doped diamond electrodes for the detection of homocysteine. Figure 4.20 showed a series of repetitive 20 μL injections of various concentrations of homocysteine in 2% acetonitrile in 0.05 M phosphate buffer (pH 2.7) at detection potential of 1.6 V. Well-defined signals without peak tailing were obtained and the current signal decreased linearly with decreasing concentration from 100 to 0.005 mM ($R^2 > 0.999$), as shown in the inset. The sensitivity, which was the slope of the plot of peak current *vs.* concentration, was 71 nA/ μM. A higher sensitivity (91 nA /μM) was also obtained when using a higher detection potential (1.8 V). The reproducibility of the response was also examined, and peak variabilities of 1.8%, 0.3% and 1.2%, respectively, were found during the course of 9 injections of 5, 1 and 0.5 μM of homocysteine (Figure 4.21). This indicated the high stability of the BDD electrode. In addition, a detection limit for S/N > 3 was determined. It was found that at 1.6 V, the anodized diamond electrode could detect a homocysteine concentration as low as 1 nM (Figure 4.25).

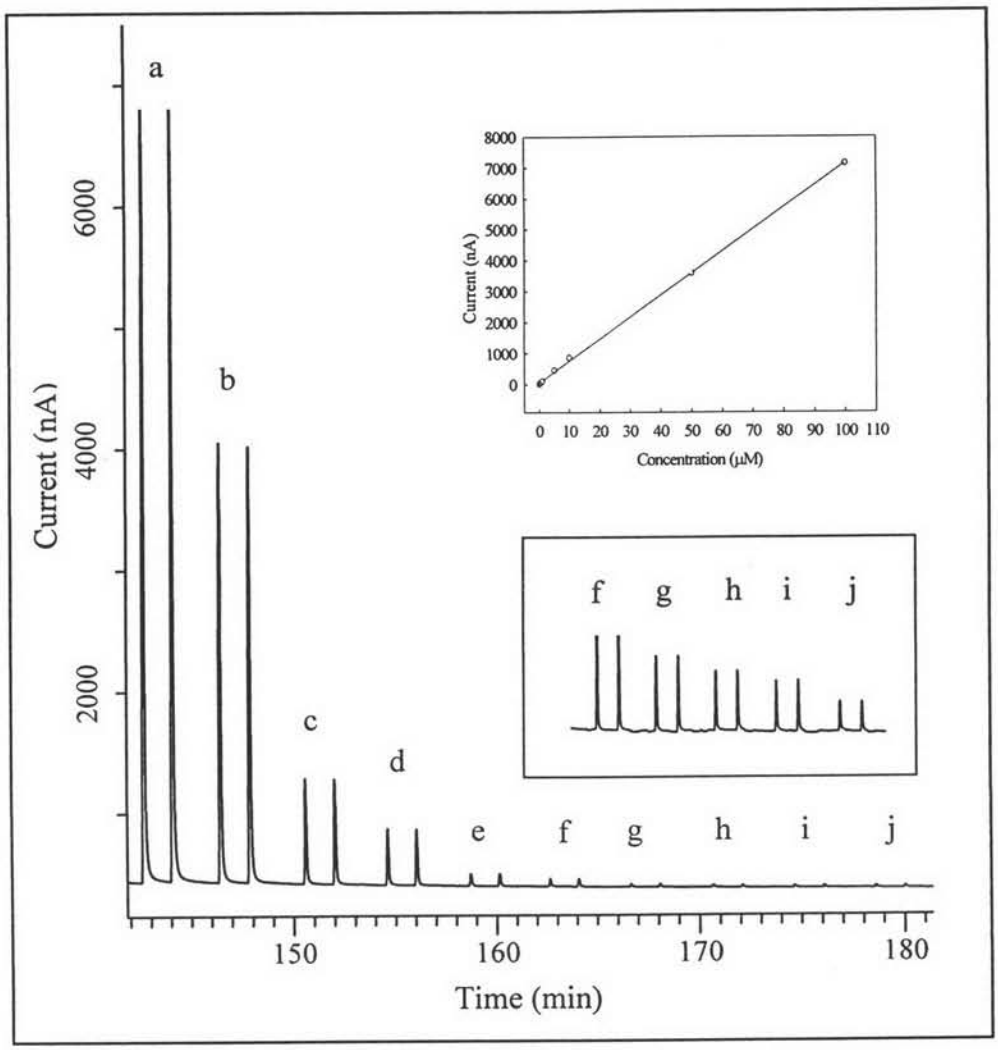

Figure 4.20 Flow injection traces with amperometric detection of homocysteine at various concentrations: a, 100 μM; b, 50 μM; c, 10 μM; d, 5 μM; e, 1 μM; f, 0.5 μM; g, 0.1 μM; h, 0.05 μM; i, 0.01 μM; and j, 0.005 μM. The calibration curve (peak current *vs.* concentration) was shown in the inset. Other conditions were the same as in Figure 4.19.

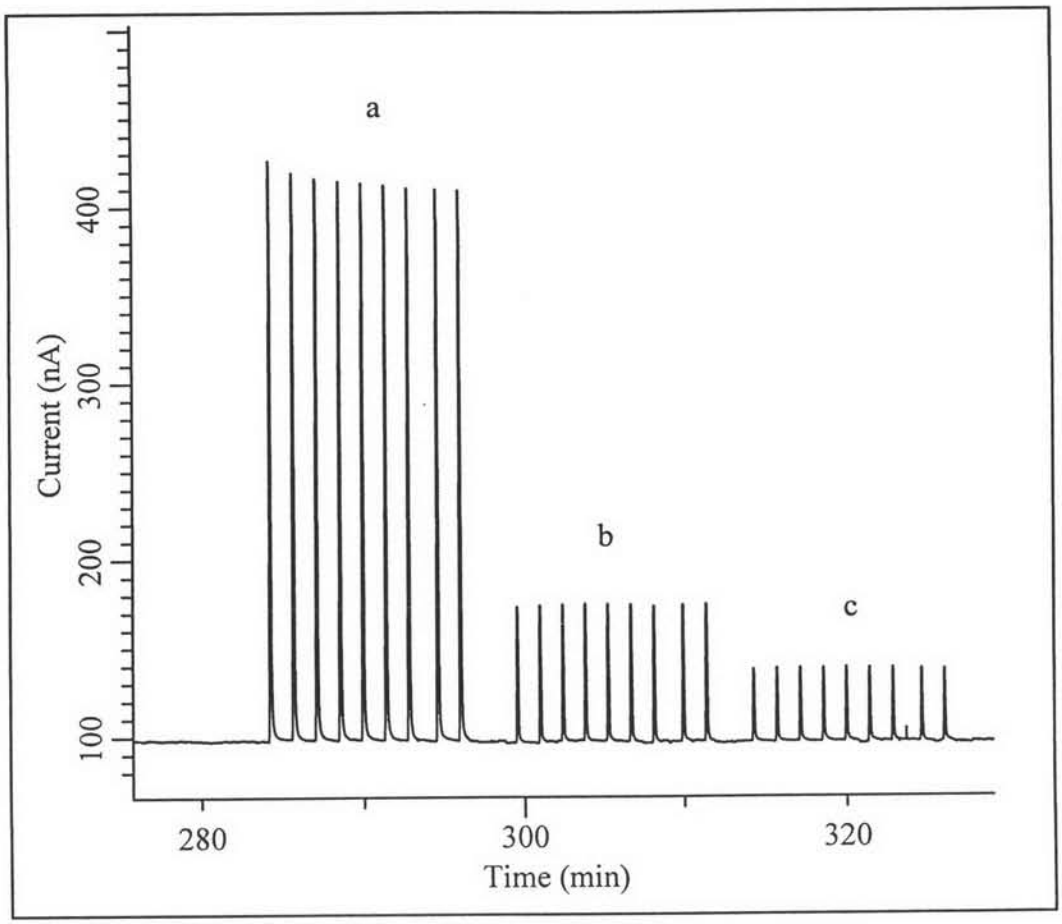

Figure 4.21 Precision results from flow injection - amperometric detection of homocysteine at concentrations of : a, 5 μM; b, 1 μM; and c, 0.5 μM (n = 9).

4.2.5 HPLC Amperometric Results

At the beginning, the experiments were conducted using the condition consisting of the ion-paring reagent OSA at the concentration of 1 mM [166] in the mobile phase (0.05 M phosphate solution, pH 2.7) at flow rate 1 mL/min. Baseline separation of seven amonothiols standard was obtained using C_{18} column. Figure 4.22 informed that a time of 65 min was required for the baseline separation of seven components due to the strong retention ability of C_{18} stationary phase towards the non-ionic organic substance.

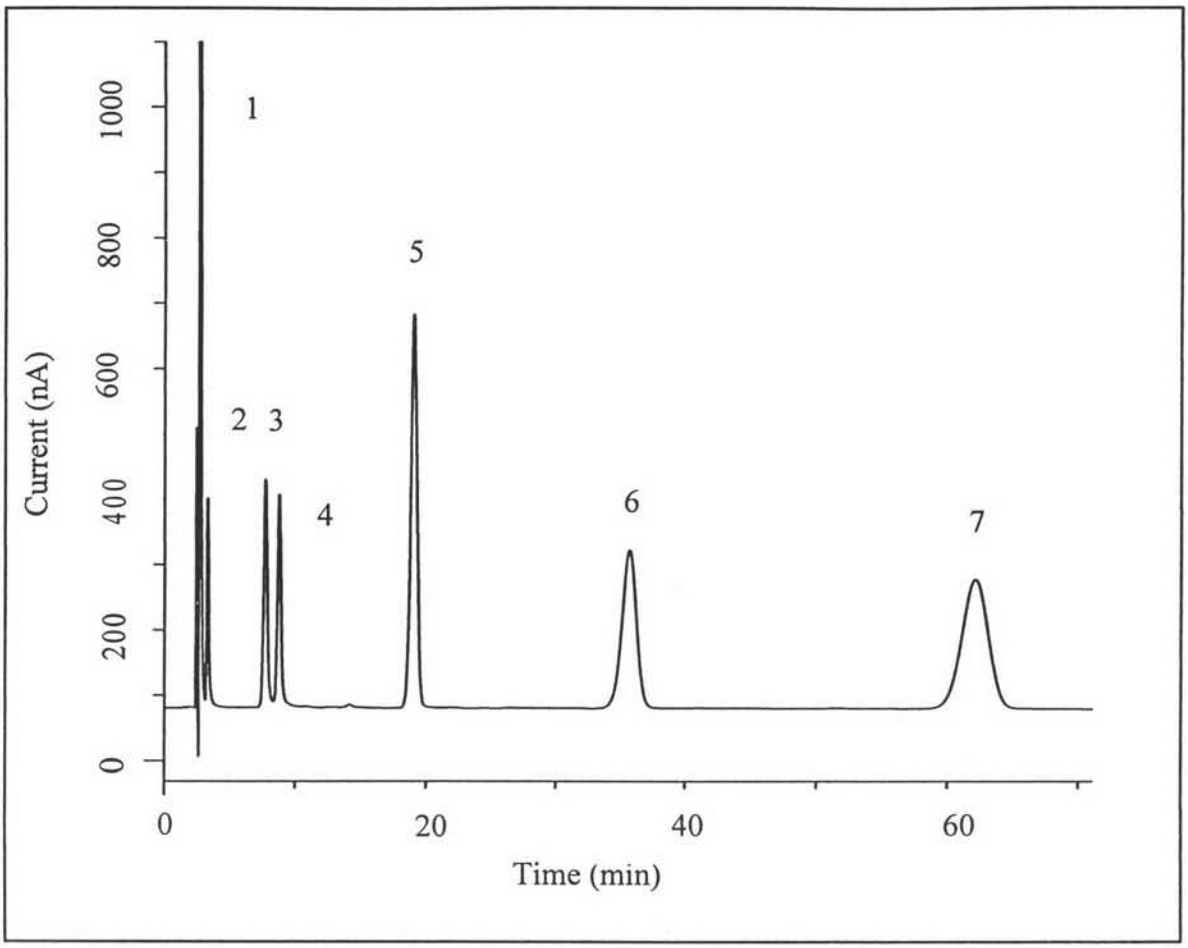

Figure 4.22 High-performance liquid chromatographic-amperometric chromatograms of aminothiols, in order of elution: 1, cystine; 2, cysteine; 3, homocysteine; 4, reduced glutathione; 5, methionine; 6, homocystine; 7, oxidized glutathione. The mobile phase was 1 mM OSA in 3% acetonitrile–0.05 M phosphate buffer (pH 2.7).

To develop the fast separation of the individual thiols, the concentration of OSA and acetronitrile was investigated. It was found that the use of lower concentration of OSA or higher concentration of acetronitrile can compromise the resolution of each aminothiols. Increasing the percent acetronitrile from 2 to 3 % did not significantly effect the retention time and the peak resolution. However, without acetronitrile, a slight increase in the capacity factor was observed, the peak widths were broadened, and therefore the resolution was worse. A minimum, 3 %, of acetronitrile in this study was needed to obtain a good resolution.

The aim of optimizing the OSA concentration was to resolve the methionine peak from the homocystine peak (Figure 4.23). Increasing the concentration of OSA increased the retention time of seven aminothilos tested. A too

high OSA concentration may result in low sensitivity, or may interfere with the electrode. The best chromatogram was achieved with the ion-pairing reagent OSA 0.2 mM in 0.05 M phosphate solution, pH 2.7 in the presence of 3% acetonitrile. At this condition, the oxidized and reduced aminothiols can be well separated at shorter retention times. Typical chromatograms of a standard solution of oxidized and reduced aminothiols are presented in Figure 4.24 and the elution times are shown in Table 4.7 The reduced aminothiols eluted within 10 min, whereas the complete profile of free oxidized thiols, including homocystine and oxidized glutathione, required 15 min.

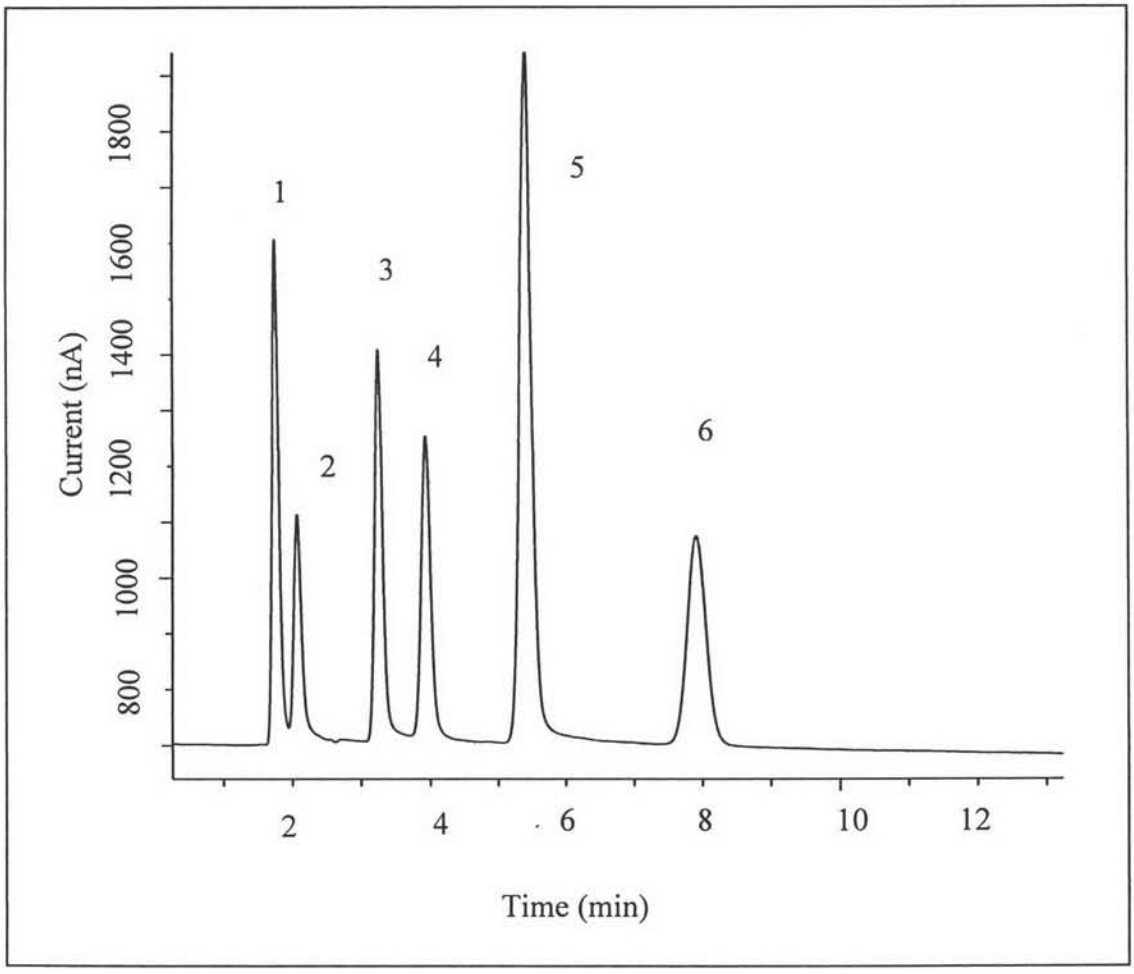

Figure 4.23 High-performance liquid chromatographic-amperometric chromatograms of aminothiols, in order of elution: 1, cystine; 2, cysteine; 3, homocysteine; 4, reduced glutathione; 5, methionine+homocystine; 6, oxidized glutathione. The mobile phase was 0.1 mM OSA in 3% acetonitrile–0.05 M phosphate buffer (pH 2.7).

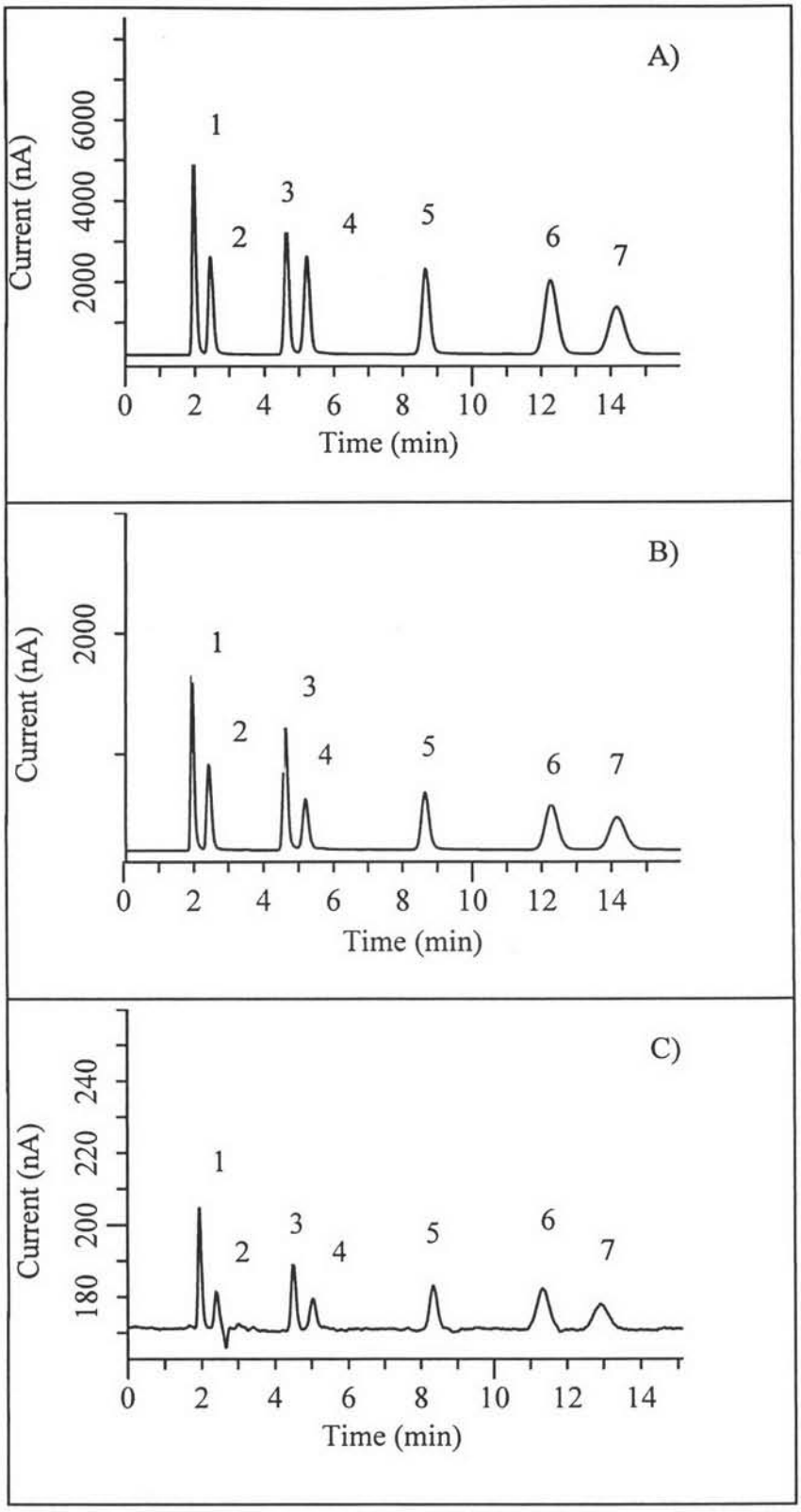

Figure 4.24 High-performance liquid chromatographic-amperometric chromatograms of aminothiols, in order of elution: 1, cystine (1.95 min); 2, cysteine (2.53 min); 3, homocysteine (4.59 min); 4, reduced glutathione (5.16 min); 5, methionine (8.50 min); 6, homocystine (12.0 min); 7, oxidized glutathione (14.20 min). The mobile phase was 0.2 mM OSA in 3% acetonitrile–0.05 M phosphate buffer (pH 2.7). (A) 100 μM, (B) 20 μM and (C) 0.5 μM.

4.2.6 Sensitivity, Detection Limit and Linear Range

As mentioned in the previoussection on hydrodynamic voltammetry, to achieve a high level of sensitivity, it was necessary to utilize a relatively high detection potential. To obtain a stable background current, it was found to be necessary to step the potential from 1 V in 0.1 V increments until 1.6 V was reached. The background current decreased gradually and needed to be stabilized before analyte injection. Regression analysis for all thiols yielded mean correlation coefficients greater than 0.99. The linear relationships between peak height (y, nA) and thiol concentration (x, μM) for each thiol wereshown in Table 4.6, together with the detection limits and linear ranges.

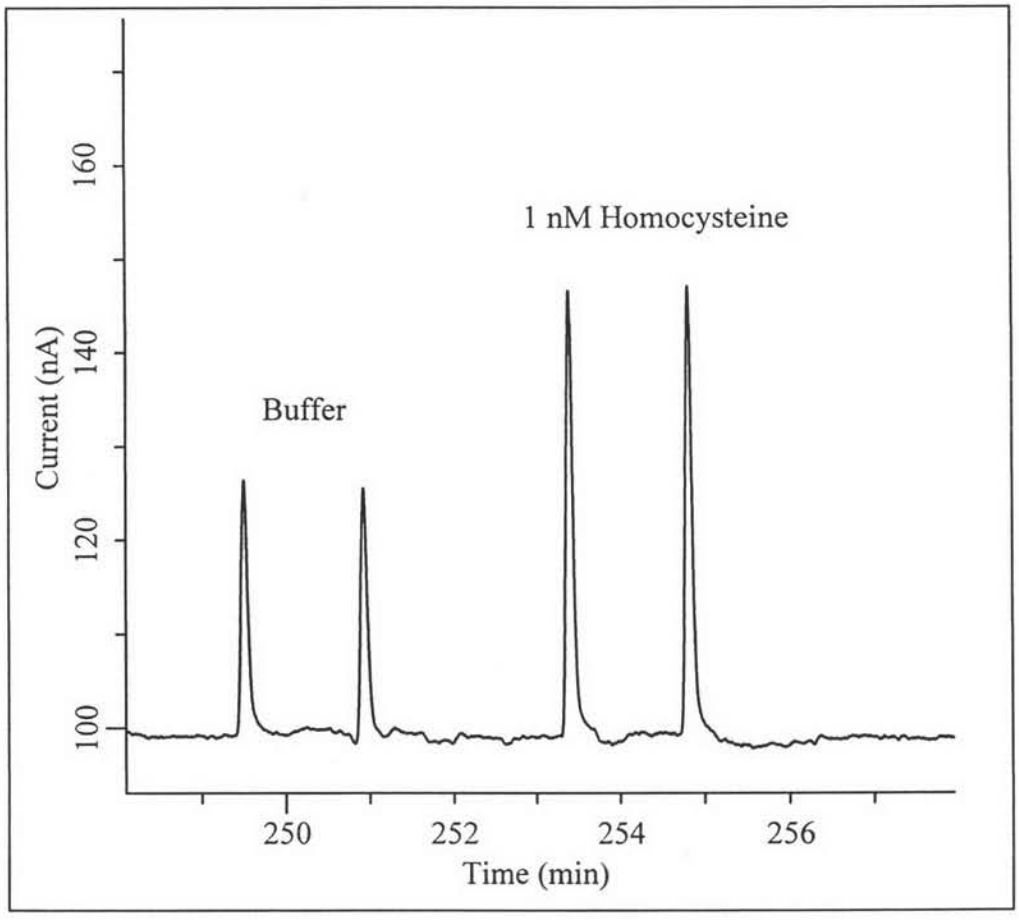

Figure 4.25 The detection limit of homocysteine from HPLC /amperometric detection at anodized boron-doped diamond thin film electrode compared to the mobile phase.

Table 4.7 Response characteristics for thiol and disulfide by HPLC amperometric detection

Compound	Elution Time / min	Linear regression line	LOD/ pmol	Linear range/μM
Cystine (Cys2)	1.95	$y = 49.016x+254.62$	1	0.05-100
Cysteine	2.53	$y = 24.325x+213.22$	1	0.05-100
Homocysteine (HCys)	4.59	$y = 32.287x+197.19$	1	0.05-100
Reduced glutathione (GSH)	5.16	$y = 24.455x+186.22$	1	0.05-100
Methionine (Met)	8.50	$y = 21.443x+187.92$	1	0.05-100
Homocystine (HCys2)	12.0	$y = 18.403x+192.24$	2	0.1-100
Oxidized glutathione (GSSG)	13.8	$y = 11.92x+185.22$	2	0.1-100

4.2.7 Summary

Homocysteine was shown to be detected directly with high sensitivity in acidic media with the use of boron-doped diamond electrodes operated in the amperometric detection mode for FIA and HPLC. Well-defined sweep rate-dependent cyclic voltammograms were obtained. The pH dependence of homocysteine oxidation shows that, at the oxidized diamond electrode, a well-defined response can be obtained both in acidic and basic media, while a response can be obtained at as-deposited diamond only in alkaline media. FIA results showed that homocysteine can be detected amperometrically with high sensitivity and reproducibility. The detection limit of 1 nM (0.02 pmol) was obtained with a response variability less than 1% (n = 9). A linear dynamic range from 0.005 to 100 μM was achieved. Well resolved chromatograms were obtained for a standard mixture of aminothiols and disulfides, indicating the feasibility for practical use in real samples, such as plasma, at anodized boron-doped diamond electrodes with an HPLC system equipped with an amperometric detector.